# Effect of Axial Growth on Turing Pattern Formation

David G. Míguez,[1] Milos Dolnik,[1] Alberto P. Muñuzuri,[2] and Lorenz Kramer[3]

[1]*Department of Chemistry and Center for Complex Systems, MS015, Brandeis University, Waltham, Massachusetts 02454-9110, USA**

[2]*Facultade de Física, Universidade de Santiago de Compostela, 15782 Santiago de Compostela, Spain*

[3]*Theoretical Physics Department, Bayreuth University, Germany*

(Received 22 September 2005; published 3 February 2006)

We have performed one-dimensional and two-dimensional experiments and simulations to study the formation of patterns in a system that grows continuously in one direction. Depending on the growth velocity, three basic spatial configurations can be obtained: stripes that are parallel, oblique, or perpendicular to the growth direction. The dependence of the wavelength on the growth velocity has also been observed. Our results illustrate the importance of these growth mechanisms in determining the final configuration of chemical and biological pattern-forming processes.

DOI: 10.1103/PhysRevLett.96.048304 PACS numbers: 82.40.Ck, 05.45.−a, 05.65.+b, 47.54.−r

Over the past decades, chemical reaction-diffusion systems have been used to model pattern formation mechanisms observed in nature [1–5]. This was Alan Turing's main focus when he launched the field more than half a century ago [6]. Turing showed that relatively simple, pure reaction-diffusion systems can produce stationary patterns in time and periodic in space [7,8]. These Turing patterns are commonly used as chemical models to understand symmetry breaking processes that occur in biology [9–15].

Living biological systems develop, change, and interact with their environment [16–18]. In the past, the majority of experimental studies on pattern formation in reaction-diffusion systems have been performed with static domains (i.e., systems with fixed sizes and fixed parameter conditions) [19–21]. But since living organisms develop under the continuous influence of external changes [22], the final shape of a living tissue (such as in somitogenesis and skin patterning) is strongly influenced by environmental variations [5,13,23,24]. The most relevant of these mechanisms is growth, which is obviously present in almost every living system [16]. The effects produced by the boundary shape and by the dynamical growth have been studied numerically and theoretically [25–30]. In this Letter, we focus on pattern formation in reaction-diffusion systems under controlled (longitudinal) axial growth in one- and two-dimensional media. We study experimentally and numerically how the growth velocity influences the wavelength of the pattern. The dependence of the spatial configuration on the velocity of the moving boundary is also reported. Our results reveal a rich, complex, and rather surprising behavior of the patterns when the boundary growth velocity is modified.

Experiments are performed using the chlorine dioxide, iodine, malonic acid (CDIMA) [31–33] reaction in a thermostated, one-sided, continuously fed unstirred reactor (CFUR) at $4 \pm 0.5\,^{\circ}\mathrm{C}$. The patterns are observed in an agarose gel (2% agarose, 0.3 mm thickness, 20 mm diameter). Reagents are fed into a continuously fed stirred tank reactor (CSTR) placed underneath the gel CFUR layer. A nitrocellulose membrane (Schleicher and Schnell, pore size 0.45 $\mu$m) and an anapore membrane impregnated with 0.5% agarose gel (Whatman, pore size 0.2 $\mu$m) are placed between the CSTR and the gel layer to avoid convection in the CFUR. Initial concentrations inside the CSTR were $[I_2]_0 = 0.45$ m$M$, $[ClO_2]_0 = 0.1$ m$M$, $[\text{poly(vinyl alcohol)}]_0 = 10$ g/l and $[H_2SO_4]_0 = 10$ m$M$, and two different concentrations for the malonic acid (MA) due to experimental requirements.

Because of the sensitivity to light of the CDIMA reaction, the effect of growth can be easily introduced into the system [34]. High light intensity suppresses the pattern and low light intensity allows Turing patterns to develop in the gel. A moving image is projected from a video projector (Hitachi CP-X327) computer controlled onto the gel (see Fig. 1). Images were recorded by a CCD camera connected to a computer for further analysis.

A typical experiment is performed as follows: at the start of the experiment, high intensity homogeneous illumination is applied to the entire system and the pattern is suppressed. Hence, the initial condition for all the experiments is the homogeneous steady state. Then the light from the video projector is blocked (masked) in a rectangular area. The size of the rectangular opaque mask image increases with time along the longitudinal direction, while the transverse dimension remains unchanged. The boundary between the illuminated and nonilluminated regions moves

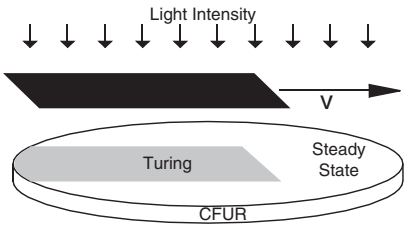


FIG. 1. Schematic of the experiment. A moving opaque mask image creates a growing shadow domain where Turing patterns can develop. In the illuminated domain the pattern is suppressed.

 

with constant velocity. Thus, the illuminated zone (with no patterns) decreases its size at the expense of the nonilluminated region (in which patterns can arise).

All the experiments shown here are performed in the absolutely unstable domain [35,36], which means that the velocity of the moving boundary of illumination ($\nu$) is smaller than the spontaneous spreading velocity of the Turing pattern, estimated as $\nu_{\text{spon}} \approx 1.8 \pm 0.1$ mm/h for the concentrations used. Under these circumstances, the pattern always arises close to the moving boundary. Ongoing experiments in the convective unstable domain reveal other interesting behavior, which is outside the scope of this Letter.

Quasi-one-dimensional experiments are performed to investigate the dependence of the wavelength of the pattern on the growth velocity in a simple configuration. For this quasi-one-dimensional experiment we use a concentration of $(\text{MA})_0 = 1$ m$M$, which produces a pattern composed of hexagonal spots with an intrinsic wavelength value of $\lambda = 0.51 \pm 0.05$ mm.

The geometry of the nonilluminated region in which patterns can form is carefully selected. In fact, the system is two dimensional but the length of one (transverse) dimension is short and fixed to be slightly larger than 1 full intrinsic wavelength of the Turing pattern. The other (longitudinal) dimension of the nonilluminated domain is continuously growing.

This geometry only allows the development of a single array of spots as shown in Fig. 2. The results of these quasi-one-dimensional experiments reveal that the wavelength of the Turing spot pattern depends on the moving boundary velocity. Figure 2(d) shows that the wavelength decreases with the growth velocity.

In the two-dimensional experiment, the fixed transverse dimension of the nonilluminated area is significantly larger than the intrinsic wavelength of the Turing patterns, and therefore the Turing patterns can develop in a full two-dimensional space. The concentration of malonic acid used in the two dimensional experiments is $(\text{MA})_0 = 1.2$ m$M$, which spontaneously produces stripes without preferential ordering [21] and with $\lambda = 0.54 \pm 0.05$ mm.

Stripes parallel to the growing axis arise in the system for relatively small values of the growth velocity [$\nu = 0.21 \pm 0.01$ mm/h in Figs. 3(a) and 3(b)]. The wavelength of the stripes is equal to the intrinsic wavelength of the spontaneously formed labyrinthine stripes, $\lambda = 0.54 \pm 0.05$ mm. The length of the stripes increases with the speed of the moving boundary.

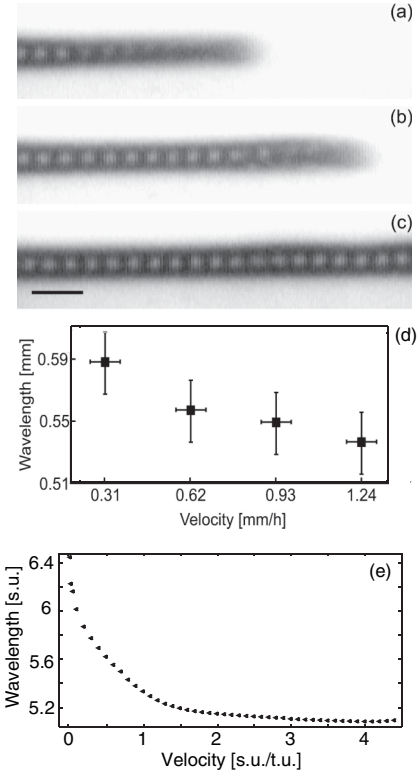


FIG. 2. Turing pattern formation in a quasi-one-dimensional system with moving boundary. (a)–(c) Snapshots of Turing patterns taken at intervals of 2 h. The shaded (nonilluminated) domain is growing from left to right. The velocity of the moving boundary is $\nu = 0.62 \pm 0.02$ mm/h The bar in (c) corresponds to 1 mm. (d) Plot of the wavelength versus the moving boundary velocity for the experiments. (e) Wavelength vs velocity for the numerical simulations in the one-dimensional system.

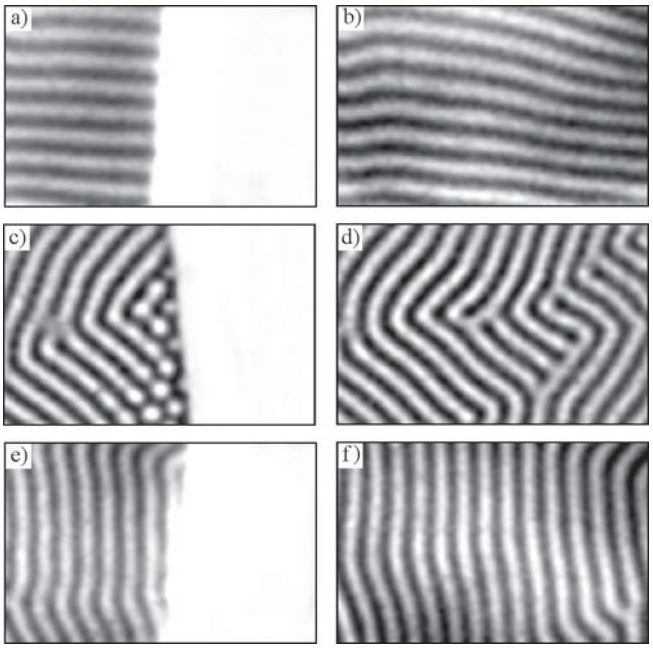


FIG. 3. Turing pattern formation in a two-dimensional system with moving boundary. Snapshots at two different times for different velocities of the moving boundary: (a),(b) $\nu = 0.21$ mm/h; (c),(d) $\nu = 0.43$ mm/h; and (e),(f) $\nu = 1.26$ mm/h. The boundary between the illuminated and nonilluminated zones moves from left to right. Size of each snapshot: $3.8 \times 6$ mm.

Intermediate values of the growth velocity ($\nu = 0.43 \pm 0.02$ mm/h) result in a new arrangement of the stripes. The pattern is composed of oblique stripes with respect to the axial direction of growth [Figs. 3(c) and 3(d)]. Figure 3(c) shows that some spots appear close to the moving boundary. These spots are not stable and the pattern relaxes to the oblique striped configuration via fusion of adjacent spots [Fig. 3(d)].

If the velocity of the moving boundary is further increased ($\nu = 1.26 \pm 0.03$ mm/h), the stripes arranged themselves perpendicular to the direction of growth and exhibit a coherent configuration [Figs. 3(e) and 3(f)]. This pattern forms by a stripe addition mechanism, with a new stripe periodically arising immediately behind the moving boundary. The wavelength dependence on the velocity is similar to that observed the quasi-one-dimensional system.

In addition, to corroborate the experimental results, one- and two-dimensional numerical simulations are performed using the Lengyel-Epstein model for the CDIMA reaction [37,38], modified to take into account the light sensitivity [34].

$$\begin{aligned} \frac{\partial u}{\partial t} &= a - cu - \frac{4uv}{1+u^2} - \phi + \nabla^2 u, \\ \frac{\partial v}{\partial t} &= \sigma\left(cu - \frac{uv}{1+u^2} + \phi + d\nabla^2 v\right). \end{aligned} \tag{1}$$

Here $u$ and $v$ are the dimensionless concentrations of the activator and the inhibitor species, respectively; $a$, $c$, and $\sigma$ are dimensionless parameters related to other initial concentrations and rate constants, and $d$ is the ratio of the inhibitor and activator diffusion coefficients. The rate of the photochemical reaction $\phi$ is a stepwise, time dependent function of the $x$-space coordinate:

$$\phi(x) = \phi_0 \quad \text{for } x < x^*(t), \tag{2}$$

$$\phi(x) = \phi_{\max} \quad \text{for } x \geq x^*(t), \tag{3}$$

$$x^*(t) = x_0 + \nu t. \tag{4}$$

The parameters used are: $a = 36$, $c = 2$, $\phi_0 = 0$, $\phi_{\max} = 5$, $d = 1.07$, $\sigma = 20$, and $x_0 = 0$. The intrinsic wavelength of the pattern is $\lambda = 5.61$ spatial units (s.u.). To mimic the experimental conditions, we set $\phi = \phi_0$ for the nonilluminated zone in which the Turing patterns can form. In the illuminated zone the term $\phi_{\max}$ results in crossing the Turing bifurcation. Hence, the steady state is the stable solution here. As in the experiment, we started with the whole medium in steady state ($\phi = \phi_{\max}$). Then, the Turing unstable domain ($\phi = \phi_0$) starts to grow from left to right. The velocity of the moving boundary $\nu$ is always less than the velocity of the spontaneous Turing pattern development. Zero flux boundary conditions are used along the static boundaries of the system.

Figure 2(e) shows the dependence of the pattern wavelength on the velocity ($\nu$) for a one-dimensional system. The results are in good agreement with the experimental results shown in Fig. 2(d). Both experimental and numerical results display decreasing pattern wavelength with increasing velocity of the moving boundary. On the other hand, the wavelength of the pattern is uniquely selected by the growth velocity among all of the unstable wavelengths predicted by simple linear stability analysis of the Turing instability. This mechanism of wavelength selection can be used to obtain the desired wavelength of an arising pattern by selecting the appropriate growth velocity.

Two-dimensional numerical simulations were performed for different velocities of the moving boundary. We found that stripes parallel to the growing axis arise in the system for small values of the system growth velocity (where t.u. stands for time units) [$\nu = 0.5$ s.u./t.u. in Fig. 4(a)]. Intermediate growth velocities [$\nu = 1.5$ s.u./t.u. in Fig. 4(b)] result in an oblique orientation of the stripes with some transient spots close to the boundary, as observed in the experiment. When the velocity of the moving boundary is further increased [$\nu = 3.0$ s.u./t.u. in Fig. 4(c)], the stripes take a perpendicular orientation to the direction of growth, in the same fashion as observed in the experiments.

To demonstrate that the pattern formation and stripe orientation are dependent only on the growth velocity, numerical simulations were also performed with stepwise changes in the moving boundary velocity [Fig. 4(d)].

A typical labyrinthlike pattern is allowed to freely develop in a rectangular domain with fixed boundaries (size $75 \times 65$ s.u.). Then at $x_0 = 65$ s.u. (i.e., the first dashed white line on the left) the right-hand boundary of illumination was allowed to move from left to right with velocity $\nu = 0.5$ s.u./t.u. The new pattern is arranged as horizontal stripes (parallel to the growth direction). Once the size of the system reached the second white dashed line at $x = x_1$,

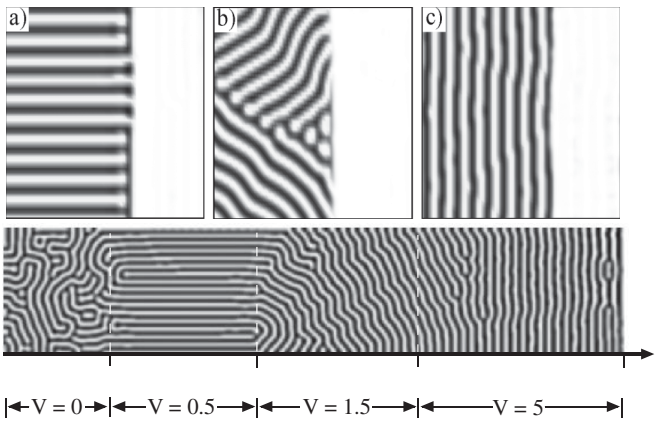


FIG. 4. Numerical simulations of Turing pattern formation in a two-dimensional system. Size of the snapshots: $55 \times 55$ s.u. Boundary moves from left to right at velocity: (a) $\nu = 0.5$ s.u./t.u., (b) $\nu = 1.5$ s.u./t.u., and (c) $\nu = 3$ s.u./t.u. (d) Turing pattern formation due to stepwise changes of the moving boundary velocity.

the velocity was increased to $\nu = 1.5$ s.u./t.u. At this velocity the newly formed pattern consists of oblique stripes, which appear after a transient. Then, at the third white dashed line at $x = x_2$, the moving boundary velocity was set to $\nu = 5$ s.u./t.u. and perpendicular stripes appear. This simulation confirms that the pattern selection is only dependent on the velocity of the moving boundary.

In this Letter we investigate Turing pattern formation in systems in which the size is allowed to grow in one direction. In a one-dimensional system the wavelength of the Turing pattern is determined by the growth velocity and decreases with the increase in the growth velocity.

In two-dimensional systems, the growth velocity acts as a selection mechanism of the final configuration of the striped pattern among three main spatial arrangements: parallel, oblique, and perpendicular stripes. Different velocity values activate different Fourier modes of the pattern. The growth axis imposes a preferential direction for the orientation of the emerging Turing pattern. The results of numerical simulation are in very good agreement with experimental observations.

In nature, the pattern formation processes and symmetry breaking phenomena often occur while the system is growing and our results illustrate the importance of the growth mechanism in the final configuration of chemical and biological pattern-forming processes.

This work has been supported by the DGI (Spain) under Project No. BFM2000-0348 and Xunta de Galicia (Spain) under Project No. PGIDT00PX120610PR and by the NSF CHE-0306262 (USA). We would like to thank Mads Kærn, Denise Tarbox, Michael Menzinger, and Irving Epstein for useful discussions and comments. All numerical computations were performed at the Centro de Supercomputación de Galicia (Spain).

*Electronic address: http://people.brandeis.edu/~miguez/
Email address: miguez@brandeis.edu

[1] H. Meinhardt, *Models of Biological Pattern Formation* (Academic, New York, 1982).
[2] A. J. Koch and H. Meinhardt, Rev. Mod. Phys. **66**, 1481 (1994).
[3] S. Kondo and R. Asai, Nature (London) **376**, 765 (1995).
[4] H. Meinhardt, *The Algorithmic Beauty of Seashells* (Springer-Verlag, Berlin, 1998).
[5] M. Kærn, D. G. Míguez, A. P. Muñuzuri, and M. Menzinger, Biophys. Chem. **110**, 231 (2004).
[6] A. M. Turing, Phil. Trans. R. Soc. B **237**, 37 (1952).
[7] V. Castets, E. Dulos, J. Boissonade, and P. de Kepper, Phys. Rev. Lett. **64**, 2953 (1990).
[8] István Lengyel and Irving R. Epstein, in *Chemical Waves and Patterns*, edited by R. Kapral and K. Showalter (Kluwer Academic, Netherlands, 1995), p. 292.
[9] A. S. Perelson, P. K. Maini, J. D. Murray, J. M. Hyman, and G. F. Oster, J. Math. Biol. **24**, 525 (1986).
[10] K. J. Painter, P. K. Maini, and H. M. Othmer, Proc. Natl. Acad. Sci. U.S.A. **96**, 5549 (1999).
[11] M. Kærn, M. Menzinger, R. Satnoianu, and A. Hunding, Faraday Discuss. **120**, 295 (2002).
[12] J. D. Murray, Sci. Am., **258** 80 (1988).
[13] J. D. Murray, *Mathematical Biology* (Springer-Verlag, Berlin, 1999).
[14] B. N. Nagorcka and J. R. Mooney, J. Theor. Biol. **98**, 575 (1982).
[15] J. H. E. Cartwright, J. Theor. Biol. **217**, 97 (2002).
[16] D. Thompson, *On Growth and Form* (Cambridge University Press, Cambridge, England, 1917).
[17] A. J. Chaplain, G. D. Singh, and J. C. McLachlan, *On Growth And Form: Spatiotemporal Pattern Formation In Biology* (John Wiley & Sons, Chichester, 1999).
[18] I. K. Quigley and D. M. Parichy, Microsc. Res. Tech. **58**, 442 (2002).
[19] Q. Ouyang, Z. Noszticzius, and H. L. Swinney, J. Phys. Chem. **96**, 6773 (1992).
[20] E. Dulos, P. Davies, B. Rudovics, and P. De Kepper, Physica D (Amsterdam) **98**, 53 (1996).
[21] Q. Ouyang and H. L. Swinney, Nature (London) **352**, 610 (1991).
[22] O. Seehausen, P. J. Mayhew, and J. J. M. van Alphen, J. Evol. Biol. **12**, 514 (1999).
[23] J. L. Aragón, C. Varea, R. A. Barrio, and P. K. Maini, FORMA **13**, 213 (1999).
[24] K. J. Painter, *IMA Volumen in Maths. & Apps* (Springer-verlag, Berlin, 2000), Vol. 121, p. 59.
[25] C. Varea, J. L. Aragón, and R. A. Barrio, Phys. Rev. E **56**, 1250 (1997).
[26] E. J. Crampin, E. A. Gaffney, and P. K. Maini, Bull. Math. Biol. **61**, 1093 (1999).
[27] E. J. Crampin and P. K. Maini, Comments on Theoretical Biology **6**, 229 (2001).
[28] E. J. Crampin, W. W. Hackborn, and P. K. Maini, Bull. Math. Biol. **64**, 747 (2002).
[29] R. G. Plaza, F. Sanchez-Garduño, P. Padilla, R. A. Barrio, and P. K. Maini, J. Dyn. Differ. Equ. **16**, 1093 (2004).
[30] P. Hantz and I. Biro, Phys. Rev. Lett. (to be published).
[31] I. Lengyel, G. Rábai, and I. R. Epstein, J. Am. Chem. Soc. **112**, 4606 (1990).
[32] I. Lengyel, G. Rábai, and I. R. Epstein, J. Am. Chem. Soc. **112**, 9104 (1990).
[33] B. Rudovics, E. Barillot, P. Davies, E. Dulos, J. Boissonade, and P. de Kepper, J. Phys. Chem. A **103**, 1790 (1999).
[34] A. P. Muñuzuri, M. Dolnik, A. M. Zhabotinsky, and I. R. Epstein, J. Am. Chem. Soc. **121**, 8065 (1999).
[35] A. B. Rovinsky and M. Menzinger, Phys. Rev. Lett. **69**, 1193 (1992).
[36] A. B. Rovinsky and M. Menzinger, in *Chemical Waves and Patterns*, edited by R. Kapral and K. Showalter (Kluwer Academic, Netherlands, 1995), p. 365.
[37] I. Lengyel and I. R. Epstein, Science **251**, 650 (1991).
[38] I. Lengyel and I. R. Epstein, Proc. Natl. Acad. Sci. U.S.A. **89**, 3977 (1992).